Localization of a Conformational Epitope Common to Non-Native and Fibrillar Immunoglobulin Light Chains†

Brian O'Nuallain, Amy Allen, Stephen J. Kennel, Deborah T. Weiss, Alan Solomon,* and Jonathan S. Wall

Human Immunology and Cancer Program, Department of Medicine, University of Tennessee Graduate School of Medicine, Knoxville, Tennessee 37920

Received August 15, 2006; Revised Manuscript Received November 20, 2006

ABSTRACT: Amyloid fibrils and partially unfolded intermediates may be distinguished serologically from native amyloidogenic precursor proteins or peptides. In this regard, we had previously reported that the IgG1 mAb 11-1F4, generated by immunizing mice with a thermally denatured variable region fragment of the human Igκ4 Bence Jones protein Len, reacted specifically with light chain (LC) fibrils, irrespective of κ or λ isotype but, notably, did not with native molecules (Hrncic, R. et al. (2000) *Am. J. Pathol. 157*, 1239−1246). To elucidate the molecular basis of this specificity, we have used a europium-linked fluorescent immunoassay, where it was demonstrated through epitope mapping that mAb 11-1F4 recognizes a conformational determinant contained within the first (N-terminal) 18 amino acids of misfolded LCs. The nature of this epitope was evidenced in competition studies where the peptide Len (1−18), but not the intact protein or other LCs, inhibited the binding of the antibody to fibrils. This unique reactivity was dependent on the structural integrity of this portion of the molecule, particularly the presence of a highly conserved prolyl residue at position 8. On the basis of our experimental data, we posit that the mAb 11-1F4 binding site found on partially denatured and fibrillar LCs involves an inducible N-terminal main chain reversal that results in the formation of a proline anchored β-turn. Our delineation of this LC fibril-associated epitope provides the rationale for the design of novel amyloid-reactive antibodies with diagnostic and therapeutic potential for patients with LC-associated and other forms of amyloidosis.

Amyloidogenesis involves a process by which normally soluble proteins or peptides form non-native intermediates that eventually assemble into fibrils (*1*). All types of amyloid, regardless of amino acid sequence, share common tertiary structural features, that is, they are comprised of extended β-sheets oriented perpendicularly to the long fibril axis (*2*, *3*) and possess sites that bind the dyes thioflavin T (ThT[1]) and Congo red (*4*, *5*). Additionally, these components and their assembly precursors, irrespective of primary structure, contain generic conformational epitopes not present on native molecules (*6*−*12*), further indicating their physical homogeneity.

The common epitopes present on amyloid fibrils and their intermediates offer targets for the design of novel diagnostic and therapeutic reagents. In this regard, we have generated a murine monoclonal antibody (mAb), designated 11-1F4 (*13*), which reacts specifically with light chain (LC) fibrils, but not soluble proteins, and has been shown in an experimental *in vivo* model to accelerate the removal of amyloidomas composed of human LC fibrils, an effect independent of the κ or λ isotype or the V_L subgroup (*9*). This mAb was generated using as immunogen a heat-aggregated suspension of the human κ4 variable domain (V_L) Len (*13*, *14*) that contained, in addition to amorphous protein aggregates, amyloid fibrils, as evidenced by Congo red staining and electron microscopy.

To localize and determine the nature of the neo-antigen recognized on conformationally altered LCs by mAb 11-1F4, we have used a highly sensitive fluoroimmunoassay to measure the interaction of this antibody with V_L peptides, as well as soluble, partially denatured, and fibrillar proteins. We now report the results of our studies that have shown, through peptide mapping, that the cryptic epitope was found within the first 18 amino acids of the V_L and was dependent on a virtually invariant prolyl residue at position 8. On the basis of the tertiary structural features of V_L Len, as evidenced by X-ray crystallography (*15*), we posit that the binding site is fixed by the presence of Pro 8 in a non-native β-turn.

MATERIALS AND METHODS

Proteins, Peptides, and Antibodies. Multiple myeloma-derived urinary and serum monoclonal Igs were isolated by zone electrophoresis on polyvinyl chloride−polyvinyl acetate blocks and, after passage through an agarose gel filtration column, their purity established by SDS−PAGE (*16*). Recombinant (r) V_κ4 Len and V_λ6 Wil were produced in E. *coli* (*17*), and the IgG1 murine monoclonal protein MOPC-

† This work was supported in part by a NIBIB/NINDS Bioengineering Research Partnership Award EB 00789, USPHS Research Grant CA 100506 from the National Cancer Institute, and the Aslan Foundation. A.S. is an American Cancer Society Clinical Research Professor.

* To whom correspondence should be addressed. Tel: 865-544-9165. Fax: 865-544-6865. E-mail: asolomon@mc.utmck.edu.

[1] Abbreviations: LC, light chains; AL, light chain-associated amyloid; ThT, thioflavin T; EuLISA, europium (Eu^{3+})-linked immunosorbant assay; V_L, light chain variable region; mAb, monoclonal antibody; PBSA, phosphate buffered saline containing 0.05% sodium azide.

10.1021/bi0616605 CCC: $37.00
Published on Web 01/10/2007

31C was purchased from Sigma (St. Louis, MO). Lyophilized components were dissolved in distilled water at a concentration of ~1 mg/mL (83 and 42 μM for rV_L and LC, respectively) and 10× PBS containing 0.05% sodium azide added in an amount sufficient to yield a final concentration of 1× (PBSA). Samples were passed through a 0.22 μm pore-size filter (Millex-GV; Millipore, Bedford, MA) and were shown by Sephadex G75 (Amersham Biosources Corp., Piscataway, NJ) gel filtration and native PAGE (NUPAGE 4−12% Bis-Tris gels, Invitrogen, Carlsbad, CA) to consist of monomers and dimers. For antibody binding studies, all LC samples were ultracentrifuged at 100,000*g* for 2 h at room temperature prior to use. Protein concentrations were determined spectrophotometrically at 280 nm using calculated molar extinction coefficients of 13,075, 24,535, and 36,120 M^{-1} cm^{-1} for V_L Wil, V_L Len, and LC Len, respectively (ExPASy, ProtParam tool). The resulting preparations were aliquoted and stored at −20 °C.

Synthetic peptides encompassing a portion or all of the 30 N-terminal amino acids of protein Len were generated by solid-phase synthesis at the Keck Biotechnology Center (Yale University, New Haven, CT) and contained acetylated N-terminal and amidated C-terminal residues (except those that had an N-terminal Asp, which was unmodified); the preparations were deemed to be 50−70% pure by mass spectrometry. The peptides were rendered aggregate-free by sequential exposure to trifluoroacetic acid and hexafluoroisopropanol (*18*), and after removal of the organic solvents by evaporation under argon, the molecules were dissolved in distilled water or, depending on the pI, in 2 mM NaOH. PBSA (10×) was added to yield a final concentration of 1× PBSA and samples centrifuged at 20,200*g* for 20 min at room temperature. Peptide fragments of V_L Len were generated by limited Asp-N proteolysis. Briefly, the protein was reduced, alkylated, and digested with endoproteinase Asp-N (Roche Applied Science, Indianapolis, IN) in 100 mM ammonium bicarbonate at pH 8.0, with an enzyme to substrate ratio of 1:100 (wt/wt) for 6 h at 37 °C. The resultant peptides were separated by HPLC and their amino acid sequences determined (Procise ABI 494 sequencer, Applied Biosystems). Peptide concentrations were measured by a bicinchoninic acid colorimetric assay (micro-BCA, Pierce, Rockford, IL) using a BSA standard curve. The samples then were used immediately.

rV_L Len fibrils were generated from the soluble precursor by agitation in an orbital shaker, as described previously (*19*). Briefly, a solution of 80 μM protein in PBSA was placed in a closed 15-mL volume polypropylene tube and shaken at 225 rpm in a 37 °C incubator. The reaction was judged complete after 2 wks when maximum ThT fluorescence occurred (*19*).

Fibrils were extracted from amyloid-laden tissues derived from patients with AL amyloidosis by the method of Pras et al. (*20*) and lyophilized. After reconstitution in PBSA, aliquots were sonicated with a probe sonic disruptor (Teledyne/Tekmar, Mason, OH), using 2 × 30 s bursts, and stored at −20 °C. Their chemical nature was determined by protein sequencing and tandem mass spectrometry (*21*).

The murine mAb 11-1F4 used in these studies was generated in a bio-reactor by the National Cancer Institute's Biopharmaceutical Development Program (SAIC-Frederick, Inc., Frederick, MD). F(ab) and $F(ab')_2$ fragments of this antibody were generated by papain and pepsin digestion, respectively, and purified as per manufacturer's recommendations (ImmunoPure kits, Pierce).

Europium-Linked Immunosorbant Assay (EuLISA). The dissociation-enhanced lanthanide fluoroimmunoassay (*22*) incorporating europium (Eu^{3+})-streptavidin and time-resolved fluorometry (DELFIA system, Perkin-Elmer Life and Analytic Sciences, Inc., Wellesly, MA) was essentially as described previously (*11*). For the binding studies, mAb 11-1F4 as well as its F(ab) and $F(ab')_2$ fragments and the isotype matched control murine monoclonal IgG1κ protein MOPC-31C were serially diluted in activated, high-binding microtiter plate wells (COSTAR, Corning, NY) that had been coated with 400−500 ng of soluble or fibrillar protein or peptide and blocked with 1% BSA in PBSA. For each competition study, the concentration of the antibody remained constant (50 or 1 nM), or the sample was serially diluted (1 μM−1 pM) in the presence of a 100−50-fold molar excess of soluble protein or 0.5−0.1 mg/mL of fibrillar protein. Biotinylated goat anti-mouse IgG or F(ab) reagents (Sigma-Aldrich, St. Louis, MO) served as the secondary antibody. After the addition of a Eu^{3+}-streptavidin conjugate followed by the releasing enhancement solution, time-resolved fluorescence was measured with a Victor^2 1420 Multilabel counter (Perkin-Elmer). The concentration of released lanthanide (fmol) was calculated from a standard curve using known amounts of Eu^{3+}. EC_{50} values (the concentration of antibody at half-maximum binding) were determined by fitting each titration data set to a sigmoid equation using the Sigma Plot 2000 v. 8 software package (SPSSN Inc., Cincinnati, OH).

In other experiments, the dose-dependent binding of mAb 11-1F4 to plate-immobilized, biotinylated and unmodified V_L Len was measured by absorbance at 405 nm using a horseradish peroxidase-conjugated goat anti-mouse IgG antibody (Sigma-Aldrich, St. Louis, MO) and 3,3′,5,5′-tetramethylbenzidine (Pierce Biotechnology, Inc., Rockford, IL) as the detection system. All microtiter plate experiments were done in triplicate; the error bars in the Figures represent the SD.

Immunohistochemistry. Four to 6 μm-thick sections were cut from formalin-fixed, paraffin-embedded blocks of amyloid-laden tissue and placed on poly-L-lysine coated microscope slides for Congo red and antibody staining. For immunohistochemistry, tissues were exposed for 1 h to a solution of 0.3−0.1 μg/mL mAb 11-1F4 in HEPES-buffered saline and then to a biotinylated sheep anti-mouse Ig antibody (MultiLink system; Biogenex, San Ramon, CA). The slides were developed using a Vector ABC kit and 3,3′-diaminobenzidene (Vector Labs, Burlingame, CA) and examined with a Leica DM500 microscope with an epifluorescent attachment. Congo red fluorescence was visualized (*23*) by use of a 540 nm bandpass filter and images acquired with a cooled CCD camera (SPOT, Diagnostic Instruments, Sterling Heights, MI).

Assurances. Studies involving human specimens were in accordance with a protocol approved by the University of Tennessee Medical Center's Institutional Review Board.

RESULTS

mAb 11-1F4 Binds to a Neo-Epitope Exposed on LC Fibrils and Partially Denatured LCs. The capability of mAb

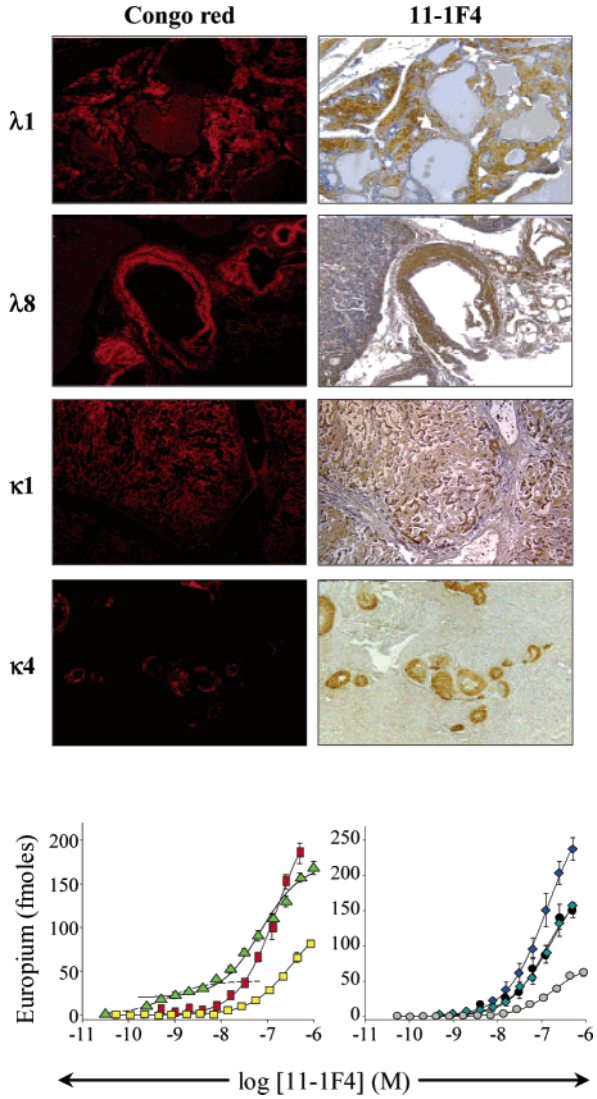

FIGURE 1: Binding of mAb 11-1F4 to LC amyloid fibrils. (Upper panel) Immunohistochemical analyses of Congo red- (left panels) and mAb 11-1F4- (right panels) stained tissue sections containing $\lambda 1$, $\lambda 8$, $\kappa 1$, and $\kappa 4$ amyloid deposits (Congo red fluorescence and immunoperoxidase reactivity, respectively; original magnification $\times 100$ ($\lambda 1$, $\lambda 8$) and $\times 80$ ($\kappa 1$, $\kappa 4$)). (Lower panel) EuLISA of mAb 11-1F4 binding to microtiter plate well-immobilized (left) $\kappa 1$ (yellow □), $\kappa 2$ (red rectangle), and $\kappa 4$ (green △), and (right) $\lambda 1$ (●), $\lambda 3$ (blue ◇), $\lambda 6$ (teal ◇), and $\lambda 8$ (gray ○) AL fibril extracts.

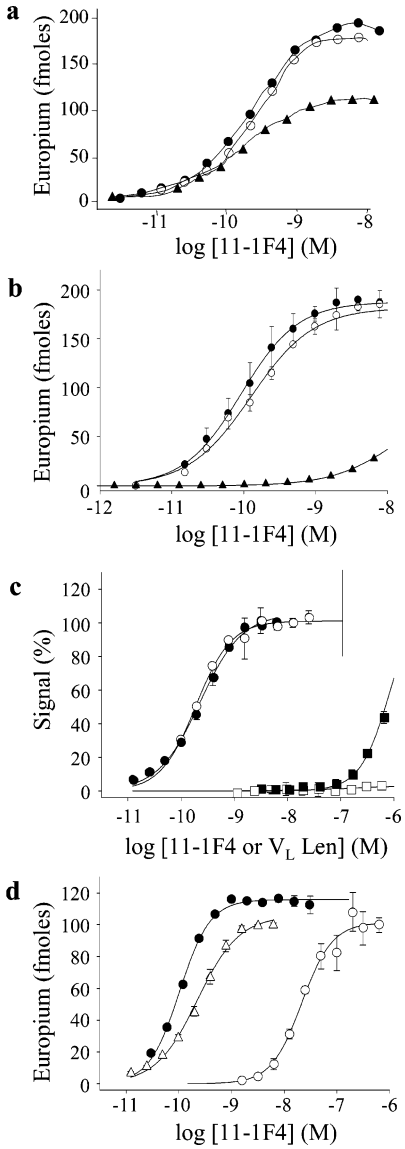

FIGURE 2: Binding of mAb 11-1F4 to native and misfolded LC molecules. Antibody interaction, measured by EuLISA, to microtiter plate well-immobilized molecules: (a) native LC Len (○), native V_L Len (●), and V_L Len fibrils (▲); (b) V_L Len in the absence (●) or presence of a 50-fold molar excess of soluble (○) or fibrillar (▲)V_L Len; (c) immobilized mAb 11-1F4 binding to uncentrifuged (■) and centrifuged (□) biotinylated V_L Len as well as solution-phase antibody binding to immobilized biotinylated (○) or unmodified V_L Len (●); (d) immobilized V_L Len in the presence of intact (△), F(ab′)$_2$ (●), and F(ab) (○) 11-1F4.

11-1F4 to recognize LC-related fibrils, regardless of their λ or κ isotype or V_L subgroup, was evidenced immunohistochemically. For example, as shown in Figure 1, this reagent immunostained $\lambda 1$-, $\lambda 8$-, $\kappa 1$-, and $\kappa 4$-related LC (i.e., AL) tissue deposits. Additionally, the specificity of mAb 11-1F4 for AL fibrils composed of different V_κ and V_λ subgroups was demonstrated by EuLISA. The EC_{50} values for binding were $\sim 130 \pm 39$ nM with an epitope density of 147 ± 65 fmol Eu^{3+}; however, in the case of $\kappa 4$ components, the curve was biphasic with EC_{50} values of ~ 0.3 and 80 nM for the higher and lower affinity sites, respectively. Presumably, this enhanced reactivity reflected the fact that $V_\kappa 4$ Len fibrils served as the 11-1F4 immunogen. In all experiments, there was no binding by the isotype-matched control antibody MOPC-31C.

The interaction of mAb 11-1F4 with microtiter plate-immobilized native and fibrillar LC Len components also was tested by EuLISA, where it was found that the antibody bound with similar avidity (EC_{50}, 0.2 ± 0.01 nM) to both types of molecules, albeit with an $\sim$2-fold reduction in signal amplitude with the fibrils (Figure 2a). To determine if the epitope recognized on native Len by mAb 11-1F4 was induced by partial denaturation resulting from microplate adsorption (rather than being present on the soluble molecule), we used a competition-based EuLISA. Notably, V_L Len fibrils markedly inhibited the binding of the antibody to plate-adsorbed V_L Len (which was ThT negative and could not promote fibrillogenesis), whereas the soluble molecule (as well as LC Len) had no effect (Figure 2b). In other experiments where mAb 11-1F4 was plate-immobilized (Figure 2c), there was no interaction with micromolar concentrations of biotinylated V_L Len that was rendered

a

Peptide or LC	Primary Sequence	EC_{50} (nM)	IC_{50} (μM)
	10 20 30		
○ LC Len	DIVMTQSPDS LAVSLGERAT INCKSSQSVL	0.18±0.03	>30.0
■ (1-30)	---------- ---------- ----------	0.21±0.04	ND
● (1-22)	---------- ---------- --	0.24±0.01	0.07±0.01
□ P8S (1-22)	---------- ---------- --	893 ±8.0	>200
▲ (1-13)	---------- ---	16.3±2.4	3.0±0.02
▲ (5-22)	------ ---------- --	36.9±1.0	20±0.7
◇ (5-15)	------ -----	>100	7.0±0.2
■ (13-24)	-------- ----	>100	>300
● (18-30)	--- ----------	>100	ND

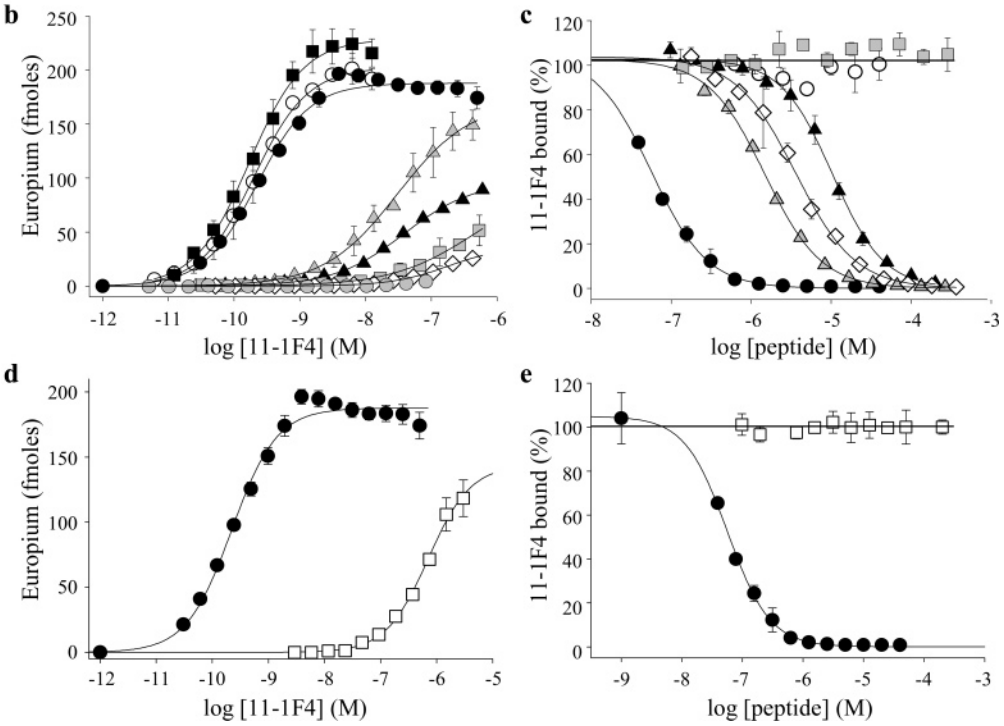

FIGURE 3: LC epitope recognized by mAb 11-1F4. (a) N-terminal amino acid sequences of the first 30 residues of LC Len and the synthetic Len-related peptides as well as the EC_{50} and IC_{50} values of antibody and peptide reactivity, respectively, determined by EuLISA from the binding and competition curves shown in panels b through e. (b) Binding of mAb 11-1F4 to microtiter plate-immobilized V_L Len and Len peptides. (c) Competition binding curves of the interaction of mAb 11-1F4 with immobilized V_L Len in the presence of V_L Len or peptides. (d) Comparison of antibody binding to immobilized Len (1−22) and the same peptide containing a serine for proline substitution at position 8 (P8S). (e) Competition binding curves of the interaction of mAb 11-1F4 with immobilized V_L Len in the presence of Len (1−22) or P8S Len (1−22) peptides.

aggregate-free by ultracentrifugation at 100,000*g* for 2 h. In contrast, the uncentrifuged material bound with an EC_{50} value of ∼1 μM. Furthermore, experiments with biotinylated and unmodified V_L Len demonstrated that biotinylation per se did not affect antibody reactivity (Figure 2c).

In studies involving heterologous κ as well as λ monoclonal LCs, it was shown that mAb 11-1F4 could only react with LC components after they were adsorbed onto microtiter plate wells and that native (soluble) forms of these molecules were incapable of inhibiting antibody binding to LC fibrils. Additionally, soluble monoclonal IgGκ4 proteins and human sera did not block the interaction of mAb 11-1F4 to V_L Len fibril-coated wells.

In other EuLISA experiments, we compared the binding to V_L Len of enzymatically obtained F(ab) and $F(ab')_2$ fragments derived from mAb 11-1F4 with that of the undigested molecule. As shown in Figure 2d, the avidities of the intact antibody and its $F(ab')_2$ derivative were virtually identical with an EC_{50} of 0.16 ± 0.14 nM, whereas this value was ∼100-fold greater for the F(ab) fragment (EC_{50}, 21.5 ± 0.1 nM).

mAb 11-1F Binds to a Conformational Epitope Located within Framework Region 1 of LCs. To identify the cryptic site on V_L Len recognized by mAb 11-1F4, the molecule was subjected to limited Asp N proteolysis. Three of the four expected peptide fragments spanning residues 1−65, 9−65, and 76−114 were obtained, purified by HPLC, immobilized on microtiter plate wells, and subjected to EuLISA, where reactivity occurred predominantly with the first. To elucidate the binding site, three overlapping synthetic peptides were generated that included residues 1−30, 22−46, and 42−65. As evidenced, the epitope recognized by this antibody was present within the first 30 amino acids, and in studies of peptides encompassing this region (Figure 3a and b), it was further localized to the N-terminal 22 residues with an EC_{50} of 0.24 ± 0.01 nM for Len (1−22),

a value comparable to that of the intact V_L (EC_{50}, 0.18 ± 0.03 nM). Notably, there was no reactivity with Len (18−30). More precisely, the structure recognized by mAb 11-1F4 was contained within the N-terminal 18 residues (EC_{50} Len (1−18), 0.30 ± 0.10 nM). That the entire 1−18 region was involved was evidenced by the finding that the EC_{50} values for Len (1−13), (5−15), and (13−24) peptides were ∼100-, 300-, and >500-fold greater, respectively, than that for Len (1−18). Additionally, the ∼200-fold weaker reactivity with Len (5−22) implied the importance of the first four N-terminal residues for antibody binding.

Whether any of these Len peptides could serve as solution-phase competitors of the interaction of mAb 11-1F4 to plate-immobilized V_L Len was also determined. With the exception of Len (5−15), the inhibitory potency of the other molecules correlated with the affinity of the antibody for the same peptides adsorbed onto microtiter plates (Figure 3b and c). However, in contrast to the relatively weak binding to plate-absorbed Len (5−15) (EC_{50} >100 nM), this peptide was a comparatively modest inhibitor with an IC_{50} of 7.0 ± 0.2 μM, a value ∼100-fold less than that of Len (1−22) (Figure 3c). Consistent with the finding that the epitope recognized by mAb 11-1F4 was not exposed on soluble rV_L Len, micromolar amounts of the native LC did not inhibit binding (IC_{50}, >30 μM) (Figure 3c). Additionally, it was shown by Western blotting that the epitope recognized by the antibody was present on surface-adsorbed monomeric V_L Len.

Given that a *cis*-proline at position 8 is found in virtually all V_κ and V_λ domains (*24*) and affects secondary structure by introducing an open turn within the framework region 1 (FR1) strand A of the LC monomer (*25*), the reactivity of mAb 11-1F4 with Len (1−22), which contained a serine substitution at position 8 (P8S), was tested by EuLISA. The mAb bound to plate-absorbed Len P8S (1−22) with an EC_{50} ∼5000-fold greater than that of Len (1−22) (Figure 3a and d). Furthermore, the soluble mutated molecule could not inhibit the binding of the antibody to plate-immobilized V_L Len (Figure 3e).

mAb 11-1F4 recognized fibrils formed from non-κ4 LCs via the same molecular mechanism as those found for protein Len, as evidenced by competition EuLISA. For example, the reaction of the antibody with fibrils formed from rV_λ6 Wil (EC_{50}, 74.6 ± 4 nM) was strongly inhibited by a 50-fold molar excess of soluble Len (1−22) (Figure 4a). Furthermore, this peptide blocked the binding of mAb 11-1F4 to amyloid fibrils composed of heterologous λ or κ proteins by more than 70%. (Figure 4b).

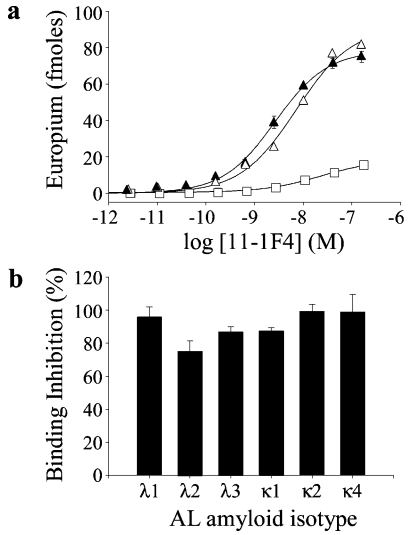

FIGURE 4: Inhibition of fibril binding by mAb 11-1F4. (a) Binding curves for the interaction of mAb 11-1F4 with microtiter plate-immobilized rV_λ6 Wil fibrils in the presence of solution-phase competitors, soluble rV_λ6 Wil (△), or Len (1−22) peptide (□), or in their absence (▲). (b) Inhibition of mAb 11-1F4 binding to human ALκ- and ALλ-related extracts by a 50× molar excess of soluble Len (1−22) peptide.

DISCUSSION

The transformation of amyloidogenic proteins or peptides into insoluble fibrils is associated with a series of conformational alterations that result in the exposure of neoantigenic sites not present on the native molecules (*6*−*12*). We have shown that the mAb 11-1F4 binds to AL amyloid and synthetic V_L fibrils irrespective of the LC isotype or V_L subgroup but not with their soluble counterparts. The inability of this reagent to react with solution−phase native LCs (relative to plate-immobilized protein) was not due to lower avidity but rather to the absence of the conformation-dependent epitope, as evidenced by the fact that antibody reactivity was not inhibited by LCs at concentrations 40,000-fold higher than the EC_{50} value obtained for the binding of a monovalent F(ab) fragment to microtiter plate-immobilized V_L Len. The relatively strong interaction of mAb 11-1F4 with partially denatured protein resulting from adsorption onto microtiter plate wells implies that epitope exposure is directly proportional to overall thermodynamic instability and, thus, the fibrillogenic potential of the V_L domain (*17*, *26*−*29*). Taken together, these data indicate that the epitope present on LC fibrils is associated with the formation of a fibril-prone structure, that is, an amyloidogenic intermediate. This conclusion is supported by the fact that mAb 11-1F4 is a potent inhibitor of *de novo* LC fibrillogenesis at sub-equimolar concentrations (*27*, *30*). The fact that the epitope also could be detected on monomeric V_L Len by Western blotting would suggest that this structure was not formed from intermolecular interfaces on an oligomeric species.

Other investigators have generated antibodies reactive with cryptic epitopes exposed on Aβ (*12*, *31*−*35*), TTR (*36*), prion (*37*, *38*), and β2-microglobulin (*39*) fibrils and assembly intermediates but not on the native precursors. For example, mAbs 39−44 and 56−61, produced against a mutant TTR molecule (G53S, E54D, and L55S), reacted with the soluble amyloidogenic variant protein but not with wild-type TTR, and as in the case of LCs, this epitope could be induced on the native protein after surface adsorption or boiling in SDS (*36*). Through peptide mapping, we have demonstrated that the mAb 11-1F4 binding site is contained within the first (N-terminal) 18 amino acids. Notably, the EC_{50} value for antibody binding to the Len (1−18) peptide was considerably less than those for the 1−13, 5−22, 5−15, 13−24, and 18−30 peptides. Additionally, residues located at positions 1−4 and those beyond 13 were found to be principally involved in the epitope recognized by this antibody. Especially critical to maintaining the integrity of this site was a Pro 8, a structural feature common to κ- and λ-type LCs (*24*, *25*).

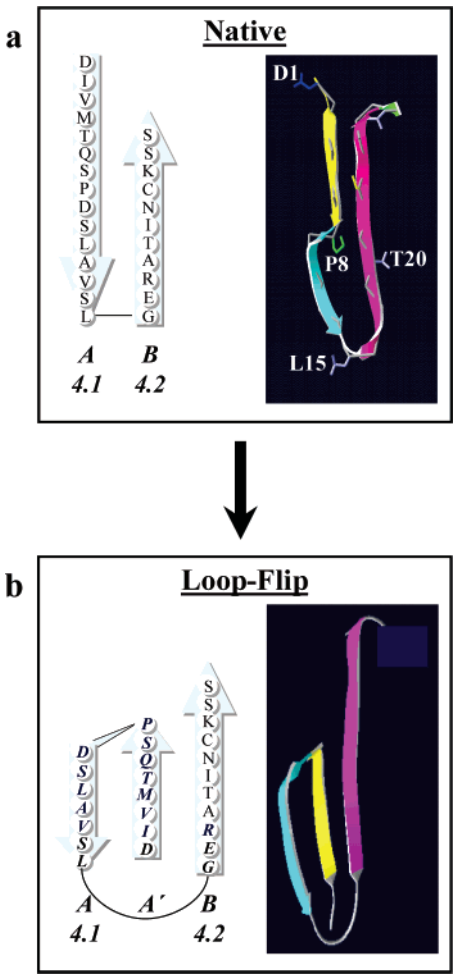

FIGURE 5: Proposed model for the conformational fibril-associated epitope recognized by mAb 11-1F4. (a) Amino acid sequence and X-ray crystallographic localization of the N-terminal A (4.1) and B (4.2) strands of native V_L Len. (b) Hypothetical structural alterations in misfolded (i.e., partially denatured or fibrillar) V_L Len involving a proline anchored loop flip of the N-terminal end of strand A (A′). The N-terminal 18 residues are bolded.

On the basis of X-ray crystallographic data on the V_L Len dimer (*15*), the N-terminal 18 residues are solvent accessible, and a *cis* Pro8 anchors a bend within strand A. Thus, we posit that the neo-epitope recognized by mAb 11-1F4 is formed from a local chain reversal that involves movement of a portion of strand A (4.1), designated A′, adjacent to strand B (4.2), following the formation of a Pro8-anchored rare type VI β turn (*40*) or a *cis*-Pro touch-turn (*41*) or, alternatively, after the isomerization of *cis*-Pro8, a type I β-turn (*42*). This chain-reversal turn-formation model would position the four N-terminal residues in close proximity to those between positions 13−18. Furthermore, the relatively large space between the C- and N-terminal ends of edge strands A and B, respectively (~8 Å), could theoretically accommodate the insertion of the A′ segment (Figure 5a and b).

Our proposed model would account for the fact that mAb 11-1F4 binds structurally perturbed LC κ4 proteins and fibrils (but not soluble native molecules) and the required participation of residues 1−4, 13−18, and Pro 8 that serve to anchor the conformational epitope. A *cis*-prolyl residue is invariably present in the third position in type VI β- and touch-turns, whereas a trans form is prevalent at position 2 in type I β-turns (*40*−*42*). Although, only ~6−10% of prolines present in proteins are in the cis configuration and <2% of β-turns are type VI (*43*), other antibodies have been found to bind conformational epitopes stabilized by such structures, for example, the HIV-neutralizing mAbs and anti-gp 41 and 120, that target envelope glycoproteins (*44*, *45*). Additionally, non-native edge strand perturbations in β_2-microglobulin involving a type I β-turn formed via a *trans*-proline are present in an amyloidogenic intermediate and have been implicated in its transition into amyloid fibrils (*46*, *47*).

The cross-reactivity of mAb 11-1F4 with fibrillar κ and λ LCs is presumably due to similar non-native chain reversals, as proposed for its binding to non-native κ4 LCs. Notably, FR1 of both isotypes has extensive sequence and structural homology, including an invariant prolyl residue at position 7 and/or 8. Although V_L Len contains a single proline at position 8 in FR1, the presence of additional prolines in this region should not affect the expression of the epitope recognized by mAb 11-1F4 because they would not hinder the formation of a rare type VI β-turn (*48*). Furthermore, mAb 11-1F4 does not react with the native Len protein that contains two solvent-exposed proline-containing β-turns (*15*), suggesting that proline, per se, is not sufficient for binding. In this regard, it is possible that the cross-reactivity of this antibody with Aβ 1−40 or 1−42 fibrils (*9*), which lack proline, results from the presence in these molecules of a putative type I β-turn (*49*, *50*).

Definitive proof of the molecular interactions of mAb 11-1F4 with misfolded LCs will require X-ray crystallographic analyses of $F(ab')_2$ 11-1F4 complexed with the Len (1−18) peptide, whereas biophysical characterization of the binding of mAb 11-1F4 to native Len (1−18) using CD, NMR, and FRET analyses could lead to further insight into the structural basis for the unique reactivity of this antibody. Future studies to determine the 3D nature of the epitope will contribute to our understanding of amyloid fibril assembly and provide a novel target for the development of antibody-based diagnostic and therapeutic agents for patients with AL amyloidosis.

ACKNOWLEDGMENT

The technical assistance of Sallie D. Macy, Craig Wooliver, Teresa K. Williams, and Charles L. Murphy and the secretarial assistance of Alisa Lehberger are gratefully acknowledged. We thank Drs. Fred J. Stevens and Allen B. Edmundson for helpful discussions.

REFERENCES

1. Dobson, C. M. (2004) Experimental investigation of protein folding and misfolding, *Methods (Orlando, Fla.) 34*, 4−14.
2. Makin, O. S., Atkins, E., Sikorski, P., Johansson, J., and Serpell, L. C. (2005) Molecular basis for amyloid fibril formation and stability, *Proc. Natl. Acad. Sci. U.S.A. 102*, 315−320.
3. Makin, O. S., and Serpell, L. C. (2005) Structures for amyloid fibrils, *FEBS. J. 272*, 5950−5961.
4. LeVine, H., III. (1993) Thioflavine T interaction with synthetic Alzheimer's disease beta-amyloid peptides: detection of amyloid aggregation in solution, *Protein Sci. 2*, 404−410.
5. Westermark, G. T., Johnson, K. H., and Westermark, P. (1999) Staining methods for identification of amyloid in tissue, *Methods Enzymol. 309*, 3−25.
6. Dumoulin, M., and Dobson, C. M. (2004) Probing the origins, diagnosis and treatment of amyloid diseases using antibodies, *Biochimie 86*, 589−600.

7. Franklin, E. C., and Zucker-Franklin, D. (1972) Antisera specific for human amyloid reactive with conformational antigens, *Proc. Soc. Exp. Biol. Med. 140*, 565−568.
8. Glabe, C. G. (2004) Conformation-dependent antibodies target diseases of protein misfolding, *Trends Biochem. Sci. 29*, 542−547.
9. Hrncic, R., Wall, J., Wolfenbarger, D. A., Murphy, C. L., Schell, M., Weiss, D. T., and Solomon, A. (2000) Antibody-mediated resolution of light chain-associated amyloid deposits, *Am. J. Pathol. 157*, 1239−1246.
10. O'Nuallain, B., and Wetzel, R. (2002) Conformational Abs recognizing a generic amyloid fibril epitope, *Proc. Natl. Acad. Sci. U.S.A. 99*, 1485−1490.
11. O'Nuallain, B., Hrncic, R., Wall, J. S., Weiss, D. T., and Solomon, A. (2006) Diagnostic and therapeutic potential of amyloid-reactive IgG antibodies contained in human sera, *J. Immunol. 176*, 7071−7078.
12. Kayed, R., Head, E., Thompson, J. L., McIntire, T. M., Milton, S. C., Cotman, C. W., and Glabe, C. G. (2003) Common structure of soluble amyloid oligomers implies common mechanism of pathogenesis, *Science 300*, 486−489.
13. Abe, M., Goto, T., Wolfenbarger, D., Weiss, D. T., and Solomon, A. (1993) Novel immunization protocol and ELISA screening methods used to obtain and characterize monoclonal antibodies specific for human light chain variable-region subgroups, *Hybridoma 12*, 475−483.
14. Schneider, M., and Hilschmann, N. (1974) The primary structure of a monoclonal immunoglobulin L-chain of kappa-type, subgroup IV (Bence-Jones protein Len). A new subgroup of the kappa-type L-chain, *Z. Physiol. Chem. 355*, 1164−1168.
15. Huang, D. B., Chang, C. H., Ainsworth, C., Johnson, G., Solomon, A., Stevens, F. J., and Schiffer, M. (1997) Variable domain structure of kappaIV human light chain Len: high homology to the murine light chain McPC603, *Mol. Immunol. 34*, 1291−1301.
16. Solomon, A. (1985) Light chains of human immunoglobulins, *Methods Enzymol. 116*, 101−121.
17. Wall, J., Schell, M., Murphy, C., Hrncic, R., Stevens, F. J., and Solomon, A. (1999) Thermodynamic instability of human lambda 6 light chains: correlation with fibrillogenicity, *Biochemistry 38*, 14101−14108.
18. O'Nuallain, B., Williams, A. D., Westermark, P., and Wetzel, R. (2004) Seeding specificity in amyloid growth induced by heterologous fibrils, *J. Biol. Chem. 279*, 17490−17499.
19. Wall, J., Murphy, C. L., and Solomon, A. (1999) In vitro immunoglobulin light chain fibrillogenesis, *Methods Enzymol. 309*, 204−217.
20. Pras, M., Schubert, M., Zucker-Franklin, D., Rimon, A., and Franklin, E. C. (1968) The characterization of soluble amyloid prepared in water, *J. Clin. Invest. 47*, 924−933.
21. Murphy, C. L., Wang, S., Williams, T., Weiss, D. T., and Solomon, A. (2006) Characterization of systemic amyloid deposits by mass spectrometry, *Methods Enzmol. 412*, 48−62.
22. Diamandis, E. P. (1988) Immunoassays with time-resolved fluorescence spectroscopy: principles and applications, *Clin. Biochem. 21*, 139−150.
23. Murphy, C. L., Eulitz, M., Hrncic, R., Sletten, K., Westermark, P., Williams, T., Macy, S. D., Wooliver, C., Wall, J., Weiss, D. T., and Solomon, A. (2001) Chemical typing of amyloid protein contained in formalin-fixed paraffin-embedded biopsy specimens, *Am. J. Clin. Pathol. 116*, 135−142.
24. Huber, R., and Steigemann, W. (1974) Two cis-prolines in the Bence-Jones protein Rei and the cis-pro-bend, *FEBS. Lett. 48*, 235−237.
25. Lefranc, M. P., and Lefranc, G. (2001) *The Immunoglobulin Facts Book*, Academic Press, London.
26. Hurle, M. R., Helms, L. R., Li, L., Chan, W., and Wetzel, R. (1994) A role for destabilizing amino acid replacements in light-chain amyloidosis, *Proc. Natl. Acad. Sci. U.S.A. 91*, 5446−5450.
27. Khurana, R., Souillac, P. O., Coats, A. C., Minert, L., Ionescu-Zanetti, C., Carter, S. A., Solomon, A., and Fink, A. L. (2003) A model for amyloid fibril formation in immunoglobulin light chains based on comparison of amyloidogenic and benign proteins and specific antibody binding, *Amyloid 10*, 97−109.
28. Raffen, R., Dieckman, L. J., Szpunar, M., Wunschl, C., Pokkuluri, P. R., Dave, P., Wilkins Stevens, P., Cai, X., Schiffer, M., and Stevens, F. J. (1999) Physicochemical consequences of amino acid variations that contribute to fibril formation by immunoglobulin light chains, *Protein Sci. 8*, 509−517.
29. Wall, J. S., Gupta, V., Wilkerson, M., Schell, M., Loris, R., Adams, P., Solomon, A., Stevens, F., and Dealwis, C. (2004) Structural basis of light chain amyloidogenicity: comparison of the thermodynamic properties, fibrillogenic potential and tertiary structural features of four Vlambda6 proteins, *J. Mol. Recognit. 17*, 323−331.
30. O'Nuallain, B., Murphy, C. L., Wolfenbarger, D. A., Kennel, S., Solomon, A., and Wall, J. S. (2005) The Amyloid-Reactive Monoclonal Antibody 11-1.F4 Binds a Cryptic Epitope of Fibrils and Partially Denatured Immunoglobulin Light Chains and Inhibits Fibrillogenesis, in *Xth International Symposium on Amyloidosis* (Grateau, G., Kyle, R. A., and Skinner, M., Eds.) pp 482−484, CRC Press, Tours, France.
31. Bard, F., Barbour, R., Cannon, C., Carretto, R., Fox, M., Games, D., Guido, T., Hoenow, K., Hu, K., Johnson-Wood, K., Khan, K., Kholodenko, D., Lee, C., Lee, M., Motter, R., Nguyen, M., Reed, A., Schenk, D., Tang, P., Vasquez, N., Seubert, P., and Yednock, T. (2003) Epitope and isotype specificities of antibodies to beta-amyloid peptide for protection against Alzheimer's disease-like neuropathology, *Proc. Natl. Acad. Sci. U.S.A. 100*, 2023−2028.
32. Hock, C., Konietzko, U., Papassotiropoulos, A., Wollmer, A., Streffer, J., von Rotz, R. C., Davey, G., Moritz, E., and Nitsch, R. M. (2002) Generation of antibodies specific for beta-amyloid by vaccination of patients with Alzheimer disease, *Nat. Med. 8*, 1270−1275.
33. Miller, D. L., Currie, J. R., Mehta, P. D., Potempska, A., Hwang, Y. W., and Wegiel, J. (2003) Humoral immune response to fibrillar beta-amyloid peptide, *Biochemistry 42*, 11682−11692.
34. Soreghan, B., Pike, C., Kayed, R., Tian, W., Milton, S., Cotman, C., and Glabe, C. G. (2002) The influence of the carboxyl terminus of the Alzheimer Abeta peptide on its conformation, aggregation, and neurotoxic properties, *NeuroMol. Med. 1*, 81−94.
35. Yang, A. J., Knauer, M., Burdick, D. A., and Glabe, C. (1995) Intracellular A beta 1-42 aggregates stimulate the accumulation of stable, insoluble amyloidogenic fragments of the amyloid precursor protein in transfected cells, *J. Biol. Chem. 270*, 14786−14792.
36. Goldsteins, G., Persson, H., Andersson, K., Olofsson, A., Dacklin, I., Edvinsson, A., Saraiva, M. J., and Lundgren, E. (1999) Exposure of cryptic epitopes on transthyretin only in amyloid and in amyloidogenic mutants, *Proc. Natl. Acad. Sci. U.S.A. 96*, 3108−3113.
37. Pan, T., Li, R., Kang, S. C., Wong, B. S., Wisniewski, T., and Sy, M. S. (2004) Epitope scanning reveals gain and loss of strain specific antibody binding epitopes associated with the conversion of normal cellular prion to scrapie prion, *J. Neurochem. 90*, 1205−1217.
38. Paramithiotis, E., Pinard, M., Lawton, T., LaBoissiere, S., Leathers, V. L., Zou, W. Q., Estey, L. A., Lamontagne, J., Lehto, M. T., Kondejewski, L. H., Francoeur, G. P., Papadopoulos, M., Haghighat, A., Spatz, S. J., Head, M., Will, R., Ironside, J., O'Rourke, K., Tonelli, Q., Ledebur, H. C., Chakrabartty, A., and Cashman, N. R. (2003) A prion protein epitope selective for the pathologically misfolded conformation, *Nat. Med. 9*, 893−899.
39. Gosal, W. S., Morten, I. J., Hewitt, E. W., Smith, D. A., Thomson, N. H., and Radford, S. E. (2005) Competing pathways determine fibril morphology in the self-assembly of beta2-microglobulin into amyloid, *J. Mol. Biol. 351*, 850−864.
40. Rose, G. D., Gierasch, L. M., and Smith, J. A. (1985) Turns in peptides and proteins, *Adv. Protein Chem. 37*, 1−109.
41. Videau, L. L., Arendall, W. B., III, and Richardson, J. S. (2004) The cis-Pro touch-turn: a rare motif preferred at functional sites, *Proteins 56*, 298−309.
42. Richardson, D. C., and Richardson, J. S. (1989) Principles and Patterns of Protein Conformation, in *Prediction of Protein Structure and the Principles of Protein Conformation* (Fasman, G.D., Ed.) pp 1−98, Plenum, New York.
43. Hutchinson, E. G., and Thornton, J. M. (1994) A revised set of potentials for beta-turn formation in proteins, *Protein Sci. 3*, 2207−2216.
44. Barbato, G., Bianchi, E., Ingallinella, P., Hurni, W. H., Miller, M. D., Ciliberto, G., Cortese, R., Bazzo, R., Shiver, J. W., and Pessi, A. (2003) Structural analysis of the epitope of the anti-HIV antibody 2F5 sheds light into its mechanism of neutralization and HIV fusion, *J. Mol. Biol. 330*, 1101−1115.
45. Tugarinov, V., Zvi, A., Levy, R., and Anglister, J. (1999) A cis proline turn linking two beta-hairpin strands in the solution

structure of an antibody-bound HIV-1IIIB V3 peptide, *Nat. Struct. Biol. 6*, 331−335.
46. Ivanova, M. I., Sawaya, M. R., Gingery, M., Attinger, A., and Eisenberg, D. (2004) An amyloid-forming segment of beta2-microglobulin suggests a molecular model for the fibril, *Proc. Natl. Acad. Sci. U.S.A. 101*, 10584−10589.
47. Jahn, T. R., Parker, M. J., Homans, S. W., and Radford, S. E. (2006) Amyloid formation under physiological conditions proceeds via a native-like folding intermediate, *Nat. Struct. Mol. Biol. 13*, 195−201.
48. Pal, D. and Chakrabarti, P. (1999) Cis peptide bonds in proteins: residues involved, their conformation, interactions and locations, *J. Mol. Biol. 294*, 271−288.
49. Makin, O. S. and Serpell, L. C. (2005) Structures for amyloid fibrils, *FEBS. J. 272*, 5950−5961.
50. Serpell, L. C. (2000) Alzhiemer's amyloid fibrils: structure and assembly, *Biochim. Biophys, Acta 1502*, 16−30.

BI0616605